

Investigation of Broadband High-Frequency Stochastic Actuation for Active-Sensing SHM Under Varying Temperature

SHABBIR AHMED and FOTIS KOPSAFTOPOULOS

ABSTRACT

The main objective of this work is the investigation and numerical assessment of random (stochastic) broadband high-frequency actuation for active-sensing structural health monitoring (SHM) via stochastic time-series models, and the comparison with traditional deterministic tone-burst actuation under varying temperature. The main hypothesis examined in this work is that random broadband actuation, within the range of 100 KHz to 1MHz, may provide additional structural information due to the excitation of additional vibration modes compared to deterministic waves with the potential cost of requiring more elaborate signal processing, modeling, and diagnostic methods. Initially, a deterministic 5-peak tone burst signal is used to excite guided-wave propagation under varying temperature in an aluminum plate outfitted with piezoelectric disk transducers. Next, the same setup is used to induce broadband high-frequency random actuation in order to enable the stochastic modeling of the structure via AutoRegressive (AR) and Functionally Pooled (FP) models. The results of the study indicate the potential of using broadband high-frequency stochastic actuation for active-sensing SHM.

INTRODUCTION

The emphasis on increased safety, enhanced reliability, and improved performance as well as to impart intelligence, such as self-sensing and self-diagnostic capabilities, in future aircraft have made it indispensable to incorporate structural health monitoring (SHM) systems into aircraft structures [1]. SHM refers to the process of damage detection, localization, and quantification which may be collectively referred to as damage diagnosis [2]. Several approaches have been proposed, such as vibration based and guided-wave based methods, with the common challenge of properly addressing varying environmental and operating conditions (EOC) [3–5].

Varying EOC, such as temperature, humidity, boundary/loading conditions and so on, may affect the structural dynamics of a system, such as the natural frequencies and damping ratios (modal parameters) [4–6] as well as the propagation of elastic/stress

Shabbir Ahmed, PhD Student, Email: ahmeds6@rpi.edu. Fotis Kopsaftopoulos, Assistant Professor, Email: kopsaf@rpi.edu. Intelligent Structural Systems Lab (ISSL), Department of Mechanical, Aerospace and Nuclear Engineering, Rensselaer Polytechnic Institute, Troy, NY, USA

waves [3, 7]. It has been reported that changes in response signals induced by the changing EOC can be of the same order of magnitude as the ones caused by damage itself, and therefore, may mask the presence of damage or hinder the damage diagnosis process [3, 8, 9]. This has been recognized as a major challenge within the SHM community and has been subject of significant research efforts in the recent years [1, 3, 5, 8, 10, 11].

When it comes to active-sensing SHM approaches, piezoelectric transducers are extremely versatile in the sense that they can be used both as actuators, i.e., generate strain from applied voltage, and sensors, i.e., generate voltage from sensed strain. In addition, piezoelectric sensors can be used to gather structural information originating from both broadband structural vibrations and narrowband acousto-ultrasonic guided waves. In the state-of-the-art SHM literature, the vast majority of guided-wave-based methods employ piezoelectric transducers to generate *deterministic* narrowband ultrasonic tone-burst waves that propagate long distances on structural components and are used for local damage detection, localization and quantification [3, 8]. Such methods are sensitive to local damage as well as EOC. On the other hand, *random* (stochastic) broadband actuation is used mainly in lower frequency ranges to enable corresponding SHM methods; the premise of such vibration-based approaches is that damage can be detected when it affects the global dynamic response of the structure [2, 5, 12]. This family of methods is less sensitive to local damage, but at the same time more robust to EOC.

The main objective of this work is the investigation and numerical assessment of random broadband high-frequency actuation for active-sensing SHM via stochastic time-series AutoRegressive (AR) and Functionally Pooled (FP) models [12, 13], and the comparison with traditional deterministic tone-burst actuation under varying temperature. The main hypothesis examined in this work is that random broadband actuation, within the range of 100 KHz to 1MHz, may provide additional structural information due to the excitation of additional vibration modes compared to deterministic waves with the potential cost of requiring more elaborate signal processing, modeling, and diagnostic methods. An additional advantage of the broadband actuation is its potential for simultaneous, rather than serial, data acquisition that may enable real-time diagnostics for SHM. According to the authors' best of knowledge, this is the first study that explores the use of random high-frequency broadband actuation for active-sensing SHM.

THE NUMERICAL MODEL, SIMULATIONS AND SIGNALS

In order to investigate and compare the high-frequency deterministic and stochastic actuation approaches, a high-fidelity Finite Element Model (FEM; ABAQUS 2018) of a thin aluminum plate was used under varying temperature (Figure 1). Three separate structural parts were created, namely the aluminum plate, adhesive, and two piezoelectric Lead Zirconate Titanate (PZT) disk transducers. For the deterministic simulations, a total time period of 0.0001 s and a time step or increment of $1e - 7$ s were used. For defining the actuation, a 5-peak-tone burst signal with a center frequency of 250 KHz was used. For the stochastic actuation, a time period of 0.0002 s and a time step of $1e - 7$ s were used with a broadband white-noise actuation frequency of 2 MHz (frequency bandwidth of 1 MHz). A detailed description of the FEM can be found in [3].

Figure 2 shows the deterministic input signal (left subplot) and the corresponding response signals (right subplot) within the 50 – 100 °C range with 5 °C increments.

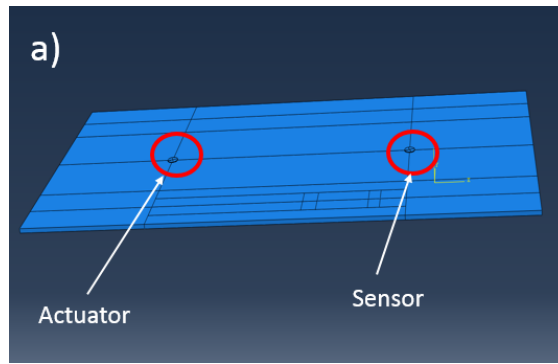


Figure 1: The FEM model used for deterministic and stochastic actuation in the temperature range (50 – 100 °C).

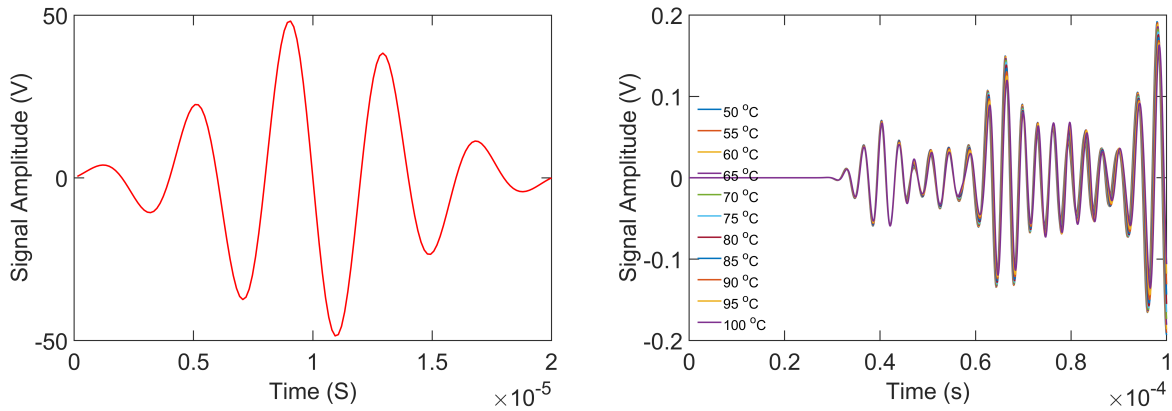


Figure 2: (left) Deterministic input, i.e. 5-peak-tone-burst, used in the FEM simulations and (right) deterministic output, i.e., guided waves, obtained from the PZT sensor for different temperatures (50 – 100 °C).

The first wave packet in the output signal ranging from 0.3 to 0.5 seconds represents the symmetric S_0 mode and the second wave packet ranging from 0.5 to 0.7 seconds represents the anti-symmetric A_0 mode.

Figure 3 (left panel) shows the magnified view of the S_0 mode. It is observed that from 50 – 75 °C, the amplitude of the S_0 mode gradually increases and reaches a peak at 75 °C. After that, from 80 – 100 °C, the amplitude starts to gradually decrease. However, in Figure 3 (right panel) which shows the magnified view of the anti-symmetric mode or A_0 mode, the amplitude of the A_0 mode gradually decreases from 50 – 100 °C. This gradual decrease may be due to the softening of the adhesive connecting the PZT to the aluminum plate. It could be further implied that the S_0 mode is less affected by this softening as the amplitude increases up to 75 °C and then decreases when the temperature is sufficiently high. However, the amplitude of the A_0 mode only decreases with the increase in temperature. In both cases, the signal shifts to the right, i.e. there is a change in time of flight of the signal due to the temperature change.

In order to gain a better understanding of the different structural states under the influence of temperature, and to properly model them, it is necessary to excite as many vibrational modes as possible. One way to perform this task is to use a broadband

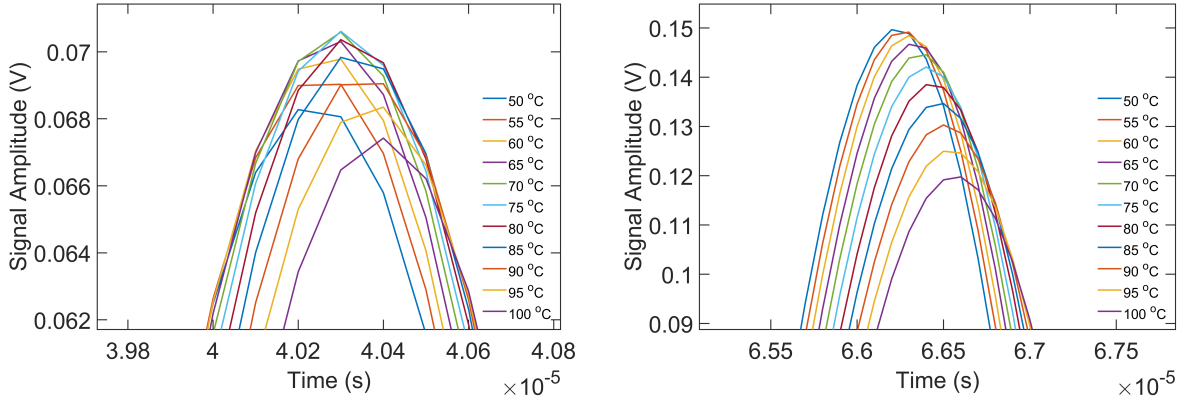


Figure 3: Close-up views of the first wave packet (S_0 mode, left panel) and second wave packet (A_0 mode, right panel) indicate the variation of the signal amplitude and phase with increasing temperature.

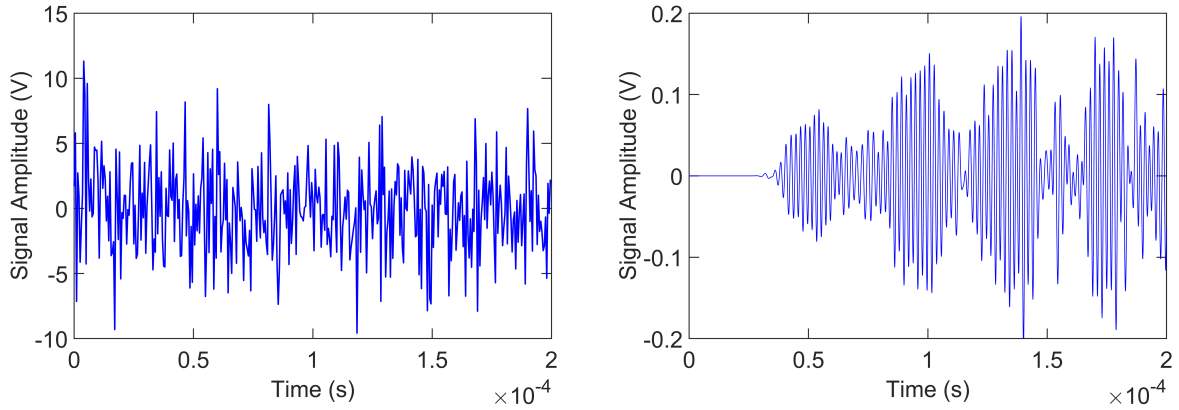


Figure 4: Representative stochastic zero-mean white noise actuation signal used in the FEM simulations (left) and corresponding PZT response signal for 25 °C (right).

random excitation signal in order to excite the vibrational modes within the bandwidth of interest. A high-frequency white-noise zero-mean signal ($\mathcal{N} \sim (0, \sigma^2)$, with $\sigma^2 = 10$) a bandwidth of 1 MHz was applied to the piezoelectric actuator and the response signal was collected from the piezoelectric sensor for different temperatures (Figure 1). The left panel in Figure 4 depicts a representative white-noise input signal while the right panel shows the corresponding output signal. A total of 16 simulations were performed from 25 °C to 100 °C with a 5 °C increment. In each case, a different white noise realization was used and the corresponding output signal was recorded in the time domain. In the next section, the modeling task under various temperatures is presented.

STOCHASTIC IDENTIFICATION UNDER VARYING TEMPERATURE

The identification of appropriate stochastic models using the available response signals under varying temperatures is considered via (i) a multi-model approach based on time-series AutoRegressive (AR) models where each model represents the dynamic re-

sponse under a *single* temperature, thus one distinct model is identified for the obtained signal under each temperature, and (ii) a “global” modeling approach that leads to single Functionally Pooled (FP) model for all considered temperatures. The advantage of this approach is that it allows for model parameters to be represented as explicit functions of the temperature.

An AR(n) model is of the following form [14]:

$$y[t] + \sum_{i=1}^n a_i \cdot y[t-i] = e[t] \quad e[t] \sim \text{iid} \mathcal{N}(0, \sigma_e^2) \quad (1)$$

with t designating the normalized discrete time ($t = 1, 2, 3, \dots$ with absolute time being $(t-1)T_s$, where T_s stands for the sampling period), $y[t]$ the measured vibration response signals as generated by the piezoelectric sensors of the structure, n the AR polynomial order, and $e[t]$ the stochastic model residual (one-step-ahead prediction error) sequence, that is a white (serially uncorrelated), Gaussian, zero mean with variance σ_e^2 sequence. The symbol $\mathcal{N}(\cdot, \cdot)$ designates Gaussian distribution with the indicated mean and variance, and iid stands for identically independently distributed.

The global FP-AR modeling involves consideration of all admissible structural states, in this case different temperatures. A total of M_1 experiments are performed (in this case via the FEM model), with M_1 designating the number of simulations under various temperatures. Each simulation is characterized by a specific temperature k^1 , with the complete series covering the required range of the variable, say $[k_{min}^1, k_{max}^1]$, via the discretizations $\{k_1^1, k_2^1, \dots, k_{M_1}^1\}$. A proper mathematical description of the global dynamics under varying structural states may then be obtained via the FP-AR(n) _{p} model of the following form [13, 15]:

$$y_k[t] + \sum_{i=1}^n a_i(k) \cdot y_k[t-i] = e_k[t] \quad (2)$$

$$e_k[t] \sim \text{iid} \mathcal{N}(0, \sigma_e^2(k)), \quad k \in \mathbb{R}, \quad E\{e_{k_i}[t] \cdot e_{k_j}[t-\tau]\} = \gamma_e(k_i, k_j) \cdot \delta[\tau] \quad (3)$$

with n designating the AR order, $y_k[t]$ the piezoelectric sensor’s response signal, and $e_k[t]$ the model’s residual (one-step-ahead prediction error) sequence, that is a white (serially uncorrelated) zero mean sequence with variance $\sigma_e^2(k)$. This may potentially be cross-correlated with its counterparts corresponding to different simulations (different k ’s). The symbol $E\{\cdot\}$ designates statistical expectation, $\delta[\tau]$ the Kronecker delta (equal to unity for $\tau = 0$ and equal to zero for $\tau \neq 0$), $\mathcal{N}(\cdot, \cdot)$ Gaussian distribution with the indicated mean and variance, and iid stands for identically independently distributed. The covariance of the residual series is designated as $\gamma_e(k_i, k_j)$, with $\gamma_e(k, k) = \sigma_e^2(k)$.

The FP model parameters $a_i(k)$ are modeled as explicit functions of temperature k :

$$a_i(k) = \sum_{j=1}^p a_{i,j} \cdot G_j(k) \quad (4)$$

with $G_i(k)$ representing the mutually independent basis functions that span the p -dimensional functional subspace determining the AR parameters [13, 16]. The FP-AR model of equations (2)–(4) is parameterized in terms of the estimated parameter vector $\theta =$

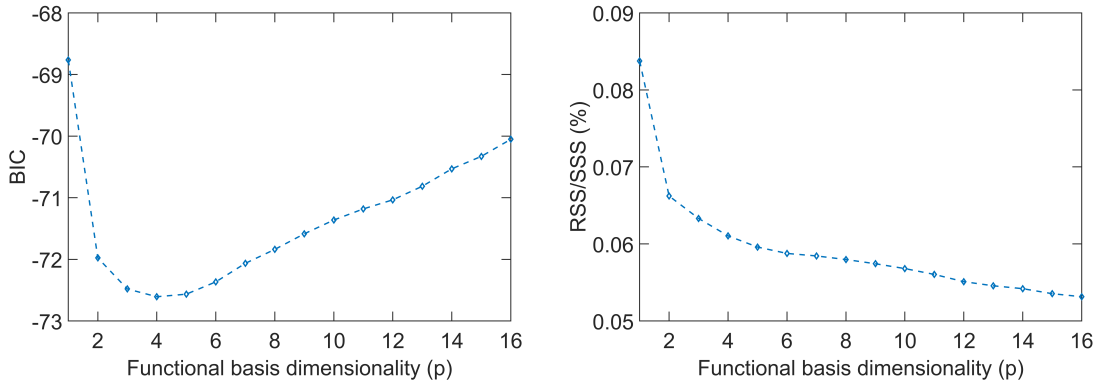


Figure 5: Functional basis selection via the BIC (left) and RSS (right) criteria.

$[a_{1,1} \ a_{1,2} \ \dots \ a_{i,j}]^T \ \forall \ k$ to be estimated from the available signals. The unknown parameter vector θ can be estimated via minimization of the Ordinary and Weighted Least Squares (OLS/WLS) criteria.

PARAMETRIC IDENTIFICATION RESULTS

The identification of the dynamics of the aluminum plate is based upon $M = 16$ sets of response data records that were collected from the PZT sensor under varying temperature. In this case, simulation datasets were collected within $[25, 100]$ °C with an increment of 5 °C. The model order selection process led to an order $n = 22$ for the AR and FP-AR models based on the Bayesian Information Criterion (BIC) and Residual Sum of Squares (RSS) over the Signal Sum of Squares (SS) criteria. Model validation took place via examination of the whiteness, or uncorrelatedness, and normality hypothesis of the model residuals. The functional subspace selection is based on the BIC and RSS/SSS criteria for increasing functional basis dimensionality. From Figure 5 it is observed that the BIC criterion yields a minimum for four basis functions. As a result, the first four Chebychev type II polynomials would be sufficient to represent the temperature dependence of the FP model parameters. From the right subplot of Figure 5, the corresponding RSS/SSS percentage is 0.062% which indicates a very accurate representation of the high-frequency plate dynamics under varying temperature by the FP model. Thus, the model identification process resulted in a FP-AR(22)₄ model.

Figure 6 depicts indicative FP model parameters. Unlike the AR parameters, FP model parameters are explicit functions of temperature. The solid blue line represents the mean parameter values and the red lines represent the ± 3 standard deviation confidence intervals. Figure 7 shows the 3D Frequency Response Function (FRF) plot based on the identified FP-AR(22)₄ model. In this case, it may be observed that the different frequencies vary smoothly with temperature. Different prominent vibrational modes for the coupled plate-adhesive-PZTs dynamic system are clearly visible and the transition of different frequencies with temperature is easily discernible. For example, it may be readily observed that the major mode is located at 520 KHz and increases with temperature. In addition, the mode at 720 KHz shows again a very clear decrease with increasing temperature.

Figure 8 presents the FRF magnitude plot for representative temperatures and their

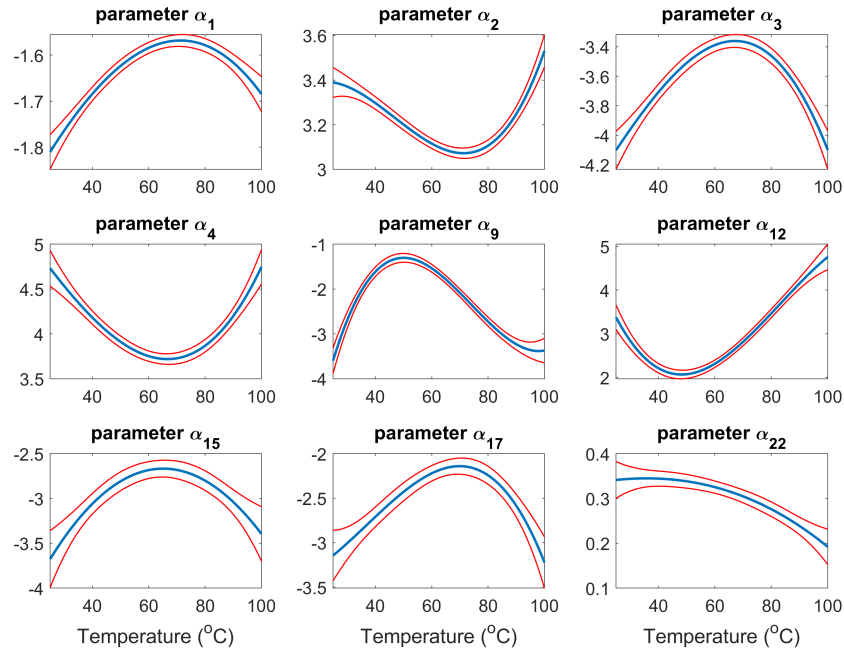


Figure 6: Indicative FP model parameter variation versus temperature. The parameter mean is shown as blue line and the associated ± 3 standard deviation as red lines.

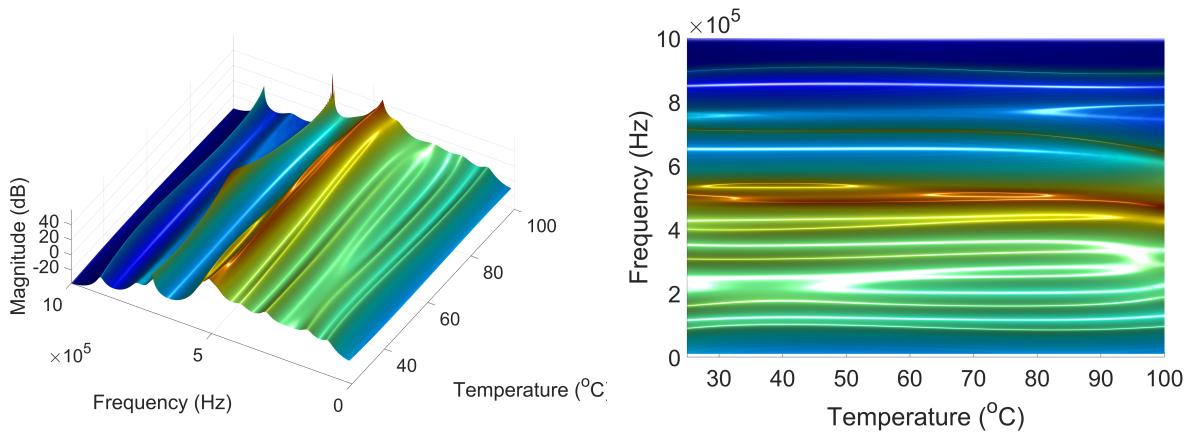


Figure 7: FRF magnitude versus temperature based on the identified FP-AR(22)₄ model.

magnified view around 0.7 MHz based on the FP-AR(22)₄ model. It may be observed that as the temperature increases within the 60 – 78 °C range, an abrupt change in magnitude occurs at 68 °C while the peak gradually shifts to lower frequencies. From 60 – 62 °C, the magnitude of the FRF gradually increases and then abruptly decreases at 68 °C. After 68 °C, the magnitude gradually decreases with increasing temperature, however there is a significant shift in frequency from 72 °C to 78 °C. In summary, the FP model can provide essential insight in the way that the system dynamics vary with temperature.

DISCUSSION AND COMPARISON

Figure 9 shows the comparison of natural frequencies for different modes versus varying temperature as identified by sixteen AR(22) (one model for each temperature)

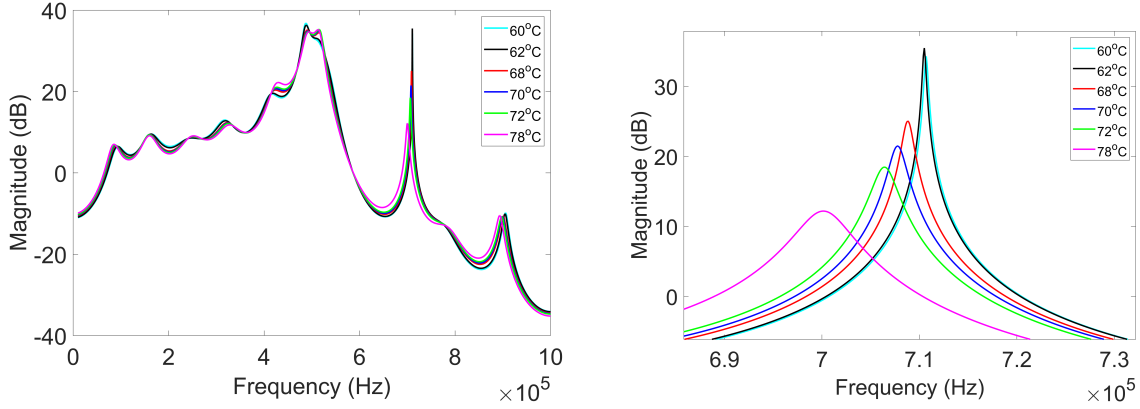


Figure 8: FRF magnitude plot based on the identified FP-AR(22)₄ model around 70 °C.

and a single FP(22)₄ model. It is observed that the natural frequencies from the multi-model AR approach oscillates with increasing temperature and they are not smooth functions of temperature. In contrast, the natural frequencies from the FP model vary smoothly, as expected, with increasing temperature. The overall trend for the FP and AR natural frequencies follow the same trend apart from the sudden fluctuations of the AR-based natural frequencies.

By comparing the deterministic trend of the 5-peak-tone-burst signals of Figure 3 with the corresponding FP-based FRF Figure 8, it may be observed that a certain similarity exists between the time-domain deterministic signal and the temperature evolution of the FP FRF magnitude based on the stochastic actuation signal. In both cases, with the increase of temperature and as the temperature reaches a certain value, an abrupt amplitude change occurs in the amplitude of the S_0 signal, with a center actuation frequency of 250 KHz, as well as in the magnitude of the FP-based FRF. As for example, the amplitude of the S_0 mode for time domain deterministic signal reaches a peak at 75 °C and then gradually decreases. Further analysis is the topic of ongoing work.

CONCLUDING REMARKS

The objective of this work was the investigation and numerical assessment of random broadband high-frequency actuation for active-sensing SHM via stochastic time-series models, and the comparison with traditional deterministic tone-burst actuation under varying temperature. The main hypothesis examined in this work is that random broadband actuation, within the range of 100 KHz to 1MHz, may provide additional structural information due to the excitation of additional vibration modes compared to deterministic waves with the potential cost of requiring more elaborate signal processing, modeling, and diagnostic methods. Deterministic 5-peak-tone burst and stochastic Gaussian white-noise actuation signals were used in an FEM of an aluminum plate outfitted with two PZT transducers under varying temperature. The random response signals were modeled based on the class of stochastic global Functionally Pooled models for representing the system dynamics under varying temperature, i.e., the model parameters are explicit functions of temperature. The FP modeling approach was compared with a multi-model

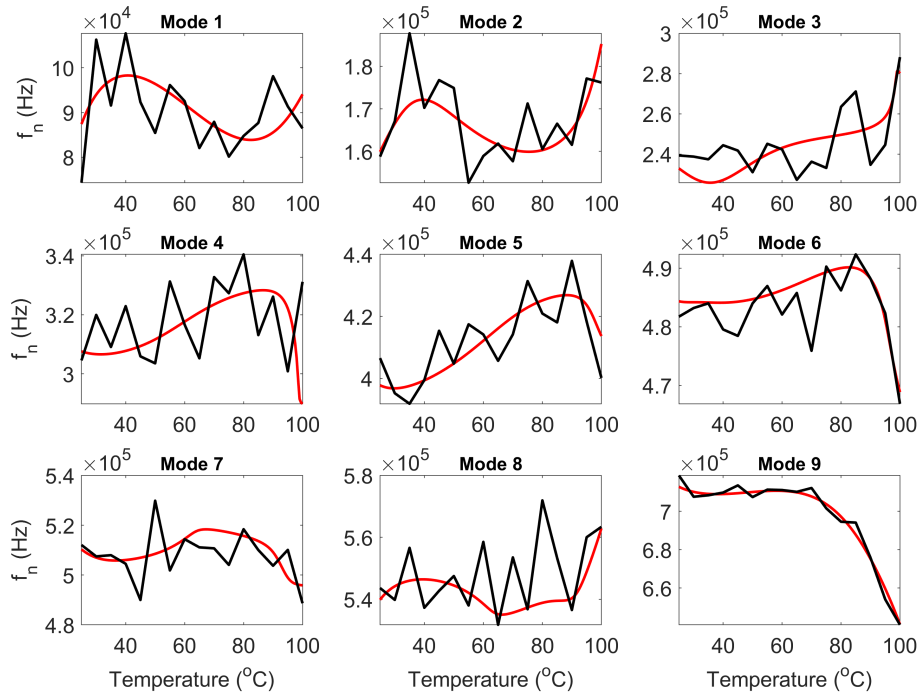


Figure 9: Comparison of natural frequencies versus temperature as identified by a single FP-AR(22)₄ (red line) and sixteen AR(22) (black line) models.

approach that is based on a parametric AR representation for each temperature. The global model offers certain advantages over the multi-model counterparts such as the simultaneous use of all available data records in a single step, and the consideration of potential cross-correlation among the data sets. In this way, the global model provides improved accuracy and more compact representations of the system dynamics under varying temperature. Finally, the trend in the amplitude and phase of the time-domain deterministic (5-peak tone burst with center actuation frequency of 250 KHz) response signals were compared with the FP parametric FRF.

Thus, it can be concluded that stochastic broadband high-frequency white-noise actuation signals and corresponding time-series modeling techniques can be employed for inferring the structural dynamic response and modal characteristics. As these models are statistical in nature, they inherently incorporate uncertainty in their prediction and may eliminate the need of computationally expensive finite element modeling.

ACKNOWLEDGMENT

This work is carried out under the support of the Army Vertical Lift Research Center of Excellence (VLRCOE) Program (W911W61120012), with Dr. Mahendra Bhagwat and Dr. William Lewis as Technical Monitors, and the U.S. Air Force Office of Scientific Research (AFOSR) grant “Formal Verification of Stochastic State Awareness for Dynamic Data-Driven Intelligent Aerospace Systems” (FA9550-19-1-0054) with Program Officer Dr. Erik Blasch.

REFERENCES

1. Kopsaftopoulos, F. and F.-K. Chang. 2018. "A Dynamic Data-Driven Stochastic State-Awareness Framework for the Next Generation of Bio-inspired Fly-by-Feel Aerospace Vehicles," in E. Blasch, S. Ravela, and A. Aved, eds., *Handbook of Dynamic Data Driven Applications Systems*, Springer International Publishing, Cham, ISBN 978-3-319-95504-9, pp. 697–721.
2. Farrar, C. R. and K. Worden. 2007. "An introduction to Structural Health Monitoring," *The Royal Society – Philosophical Transactions: Mathematical, Physical and Engineering Sciences*, 365:303–315.
3. Ahmed, S. and F. P. Kopsaftopoulos. 2019. "Uncertainty quantification of guided waves propagation for active sensing structural health monitoring," in *Proceedings of the Vertical Flight Society 75th Annual Forum & Technology Display*, Philadelphia, PA, USA.
4. Hios, J. D. and S. D. Fassois. 2009. "Stochastic identification of temperature effects on the dynamics of a smart composite beam: assessment of multi-model and global model approaches," *Smart Materials and Structures*, 18(3):035011.
5. Avendaño-Valencia, L. D., E. N. Chatzi, K. Y. Koo, and J. M. Brownjohn. 2017. "Gaussian Process time-series models for structures under operational variability," *Frontiers in Built Environment*, 3:69.
6. Moser, P. and B. Moaveni. 2011. "Environmental effects on the identified natural frequencies of the Dowling Hall Footbridge," *Mechanical Systems and Signal Processing*, 25(7):2336–2357.
7. Janapati, V., F. Kopsaftopoulos, F. Li, S. Lee, and F.-K. Chang. 2016. "Damage detection sensitivity characterization of acousto-ultrasound-based structural health monitoring techniques," *Structural Health Monitoring*, 15(2):143–161.
8. Janapati, V., F. Kopsaftopoulos, F. Li, S. J. Lee, and F.-K. Chang. 2016. "Damage detection sensitivity characterization of acousto-ultrasound-based structural health monitoring techniques," *Structural Health Monitoring*, 15(2):143–161.
9. Konstantinidis, G., B. Drinkwater, and P. Wilcox. 2006. "The temperature stability of guided wave structural health monitoring systems," *Smart Materials and Structures*, 15(4):967.
10. Sohn, H. 2006. "Effects of environmental and operational variability on structural health monitoring," *Philosophical Transactions of the Royal Society A: Mathematical, Physical and Engineering Sciences*, 365(1851):539–560.
11. Amer, A. and F. P. Kopsaftopoulos. 2019. "Probabilistic active sensing acousto-ultrasound SHM based on non-parametric stochastic representations," in *Proceedings of the Vertical Flight Society 75th Annual Forum & Technology Display*, Philadelphia, PA, USA.
12. Kopsaftopoulos, F. P. and S. D. Fassois. 2013. "A Stochastic Functional Model Based Method for Vibration Based Damage Detection, Localization, and Magnitude Estimation," *Mechanical Systems and Signal Processing*, 39(1–2):143–161.
13. Sakellariou, J. S. and S. D. Fassois. 2016. "Functionally Pooled models for the global identification of stochastic systems under different pseudo-static operating conditions," *Mechanical Systems and Signal Processing*, 72-73:785807, doi:10.1016/j.ymssp.2015.10.018.
14. Ljung, L. 1999. *System Identification: Theory for the User*, Prentice-Hall, 2nd edn.
15. Kopsaftopoulos, F., R. Nardari, Y.-H. Li, and F.-K. Chang. 2018. "A stochastic global identification framework for aerospace structures operating under varying flight states," *Mechanical Systems and Signal Processing*, 98:425–447.
16. Kopsaftopoulos, F. P. 2012. *Advanced Functional and Sequential Statistical Time Series Methods for Damage Diagnosis in Mechanical Structures*, Ph.D. thesis, Department of Mechanical Engineering & Aeronautics, University of Patras, Patras, Greece.